British Journal of Cancer www.nature.com/bjc

ARTICLE

Cellular and Molecular Biology

CD20 expression, TrkB activation and functional activity of diffuse large B cell lymphoma-derived small extracellular vesicles

Marine Aitamer[1], Hussein Akil[1], Chantal Vignoles[1], Maud Branchaud[2], Julie Abraham[1,3], Nathalie Gachard[1,4], Jean Feuillard[1,4], Marie-Odile Jauberteau[2], Hamasseh Shirvani[5], Danielle Troutaud[1,6]✉ and Hafidha Bentayeb[2,6]

BACKGROUND: Small extracellular vesicles (sEVs) including exosomes, carrying the CD20, could be involved in immunotherapy resistance in diffuse large B cell lymphoma (DLBCL). We have reported endogenous brain-derived neurotrophic factor/TrkB (tropomyosin-related kinase B) survival axis in DLBCL. Here, we performed a comparative study of sEV production by germinal centre B cell (GCB) and activated B cell (ABC)-DLBCL cell lines, and analysed TrkB activation on this process.
METHODS: GCB (SUDHL4 and SUDHL6) and ABC (OCI-LY3, OCI-LY10 and U2932) cell lines were used. sEVs were characterised using nanoparticle tracking analysis technology and western blot. CD20 content was also analysed by enzyme-linked immunoassay, and complement-dependent cytotoxicity of rituximab was investigated. 7,8-Dihydroxyflavone (7,8-DHF) was used as a TrkB agonist. In vivo role of sEVs was evaluated in a xenograft model.
RESULTS: sEVs production varied significantly between DLBCL cells, independently of subtype. CD20 level was consistent with that of parental cells. Higher CD20 expression was found in sEVs after TrkB activation, with a trend in increasing their concentration. sEVs determined in vitro and in vivo protection from rituximab, which seemed CD20 level-dependent; the protection was enhanced when sEVs were produced by 7,8-DHF-treated cells.
CONCLUSIONS: DLBCL-derived sEVs have the differential capacity to interfere with immunotherapy, which could be enhanced by growth factors like neurotrophins. Evaluating the sEV CD20 level could be useful for disease monitoring.

British Journal of Cancer (2021) 125:1687–1698; https://doi.org/10.1038/s41416-021-01611-7

BACKGROUND

Diffuse large B cell lymphoma (DLBCL) is the most common subtype of non-Hodgkin lymphoma (NHL), accounting for 30–40% of all newly diagnosed cases worldwide. DLBCL is a highly aggressive and heterogeneous lymphoma that would imminently be fatal without treatment. Two major prognostically significant subtypes have been identified, which differ from the cell origin, germinal centre B cell (GCB) and activated B cell (ABC) type of better and worse prognostic, respectively [1–3]. A monoclonal anti-CD20 antibody, rituximab (Rtx), combined with CHOP chemotherapy (R-CHOP immunochemotherapy) has been widely used with favourable results and is still the standard treatment for several kinds of B-NHL, including DLBCL. However, 30–40% of patients are not cured and will relapse or be refractory to R-CHOP. Thus, primary or acquired resistance to Rtx has become a considerable problem [4–6]. Several mechanisms of resistance have been predicted, but their clinical significance remains unclear. However, decreased CD20 expression has been postulated to be one of the most important etiologies contributing to Rtx resistance. Indeed, CD20 level determined by flow cytometry at onset is an independent predictor for the prognosis of patients with DLBCL [7]. Moreover, a CD20-negative ($CD20^-$) phenotypic transformation was observed in patients after Rtx treatment, and in B-lymphoma cells Rtx was shown to down-regulate CD20 gene (*MS4A1*) expression partially by using epigenetic mechanisms [8–10]. Thus, targeting the modulation of CD20 membrane expression, which represents a key factor in determining anti-CD20 effectiveness, is still an important challenge for novel therapy in combination with immunotherapy in B cell neoplasms.

Exosomes are small extracellular vesicles (sEVs) of endosomal origin ranging from 50 to 150 nm and secreted by several cell types during exocytic fusion of multivesicular bodies (MVB) with the plasma membrane [11, 12]. In physiologic conditions, exosomes are released by erythroid progenitors during their maturation process, as well as by B-lymphocytes and dendritic

[1]UMR CNRS 7276/INSERM U1262, Faculté de Médecine, Université de Limoges, 2 rue du Docteur Marcland, 87025 Limoges, Cedex, France. [2]EA3842 CAPTuR Facultés de Médecine et de Pharmacie, Université de Limoges, 2 rue du Docteur Marcland, 87025 Limoges, Cedex, France. [3]Service d'Hématologie Clinique, CHU de Limoges, 2 Avenue Martin Luther King, 87000 Limoges, France. [4]Laboratoire d'hématologie, CHU de Limoges, 2 Avenue Martin Luther King, 87000 Limoges, France. [5]Institut Roche, 30, cours de l'île Seguin, 92650 Boulogne-Billancourt, France. [6]These authors contributed equally: Danielle Troutaud, Hafidha Bentayeb. ✉email: danielle.troutaud@unilim.fr

Received: 3 August 2021 Revised: 19 September 2021 Accepted: 21 October 2021
Published online: 6 November 2021

cells. Exosomes were shown to play multiple immunomodulatory functions, which leads to multiple studies and clinical trials as tumour "vaccines". Importantly, many cancer cells have been shown to secrete exosomes in greater amounts than normal cells [13, 14], and as exosome composition seems to be cell- and tissue-specific, they are highly suitable to serve as diagnostic markers. Current knowledge of tumour-derived exosomes suggests that they can also play an important role in the development and progression of cancer [15]. They can modulate intercellular communication within the tumour microenvironment by the transfer of multiple signalling molecules like protein, lipid and RNA cargo [16–18]. In DLBCL, increasing evidence supports a role for sEVs in progression and response or resistance to therapy. sEV-containing CD20 could shield target cells from anti-CD20 antibody attack, revealing a possible role of resistance to immunotherapy in DLBCL patients [19]. Similarly, DLBCL-derived exosomes attenuated chemotherapeutic efficacy by encapsulating doxorubicin and removing it from the cells [20]. Interestingly, recent data showed that RNA contents of peripheral sEVs from DLBCL patients could enable disease monitoring through liquid biopsy [21] and can be used as predictors of prognosis and chemotherapeutic efficacy [22]. However, biological stimuli regulating quantitatively and/or qualitatively exosome secretion remain poorly defined, notably in a comparative study on GCB and ABC subtypes and after Rtx exposure.

Neurotrophins (NTs) along with the brain-derived neurotrophic factor (BDNF) are structurally and functionally related growth factors widely expressed in a variety of tissues including the immune system [23]. Moreover, NTs and their Trk (tropomyosin-related kinase) receptors are involved by autocrine and/or paracrine signalling pathways in cancer cell growth and dissemination [24]. The binding of BDNF to its high-affinity receptor TrkB triggers cell survival by activating several signalling pathways (PI3K/Akt, MAPK, and PLC-γ). We have previously demonstrated that BDNF can realise autocrine/paracrine loops involved in the survival of human DLBCL cell lines. Furthermore, inhibition of Trk signalling induced cell apoptosis and potentiated the cytotoxic effect of Rtx in vitro and in vivo [25, 26]. We hypothesised that BDNF/TrkB signalling could interfere with Rtx sensitivity and thus may contribute to therapeutic resistance.

The objective of this work was to realise a comparative study of sEVs derived from GCB and ABC-DLBCL cell lines, by analysing CD20 content in relation to its ability to protect cells from Rtx-induced cytotoxicity. Furthermore, we explored the effect of 7,8-dihydroxyflavone (7,8-DHF), a TrkB agonist [27], on sEV secretion and CD20 expression in comparison to Rtx exposure. The in vitro (DLBCL cell lines) and in vivo (GCB-DLBCL xenograft model in severe combined immunodeficiency (SCID) mice) findings discussed in this study strongly argue for the role of sEVs, including exosomes, in the immunotherapy escape of DLBCL tumour cells. Furthermore, they may improve our understanding of the molecular events leading to the expression of CD20 at the cellular and sEV levels.

MATERIALS AND METHODS

Human B cell lines and cell cultures

Two GCB-DLBCL cell lines (SUDHL4 and SUDHL6 obtained from DSMZ) and three ABC-DLBCL cell lines (OCI-LY3 and OCI-LY10, given by Pr. Feuillard, UMR CNRS 7276, Limoges University, with the kind agreement of the Louis M. Staudt, National Cancer Institute, USA and U2932 from DSMZ) were used. The cell lines were grown in RPMI-1640 medium (Lonza) supplemented with 10% heat-inactivated foetal bovine serum (FBS) (Hyclone), 100 U/mL penicillin and 100 µg/mL streptomycin (Gibco) at 37 °C in a humidified atmosphere containing 5% CO_2. Cell lines were expanded upon receipt and low-passage vials were stored in liquid nitrogen. All experiments were realised within 8 weeks after drawing. The cell lines were routinely tested to confirm the absence of mycoplasma by the MycoAlert Kit from Lonza. For the functional analyses, cells (10^6/mL) were incubated with Rtx (MabThera®, stock 10 mg/mL, a generous gift from CHRU Dupuytren of Limoges, Pharmacie centrale) and 7,8-DHF (500 nM, Sigma-Aldrich, France) or exogenous BDNF (rhBDNF, 100 ng/mL, Promega) alone or in combination.

Flow cytometry analysis of surface and intracellular CD20 expression

After washing in phosphate-buffered saline (PBS), 0.5×10^6 DLBCL cells were used for cytometry analysis of surface CD20 expression using PE-labelled mouse anti-CD20 antibody (clone B9E9 [HRC20]; Beckman Coulter) incubated for 30 min at 4 °C to detect the extracellular epitope located in the larger CD20 loop. Isotypic control was also realised (IgG2a mouse-PE, Beckman Coulter). After washing, cells were resuspended in PBS/1% formaldehyde. $CD20^+$ cells were analysed with a FACSCalibur flow cytometer (Becton Dickinson, Heidelberg, Germany) acquiring 10,000 events after gating on light scatter properties (forward vs side: FSC/SSC) to eliminate debris and cellular aggregates. The mean fluorescence intensity (MFI) values were used as a semiquantitative measure of the expression of CD20.

Alternatively, when cells were exposed to treatment (i.e. Rtx or 7,8-DHF), they were fixed in PBS with 1% formaldehyde, permeablized with ice-cold 100% methanol for 20 min at −20 °C, washed in PBS and incubated with 3% bovine serum albumin (BSA)-PBS for 30 min at 4 °C. Then, cells were incubated for 1 h at 4 °C with rabbit anti-CD20 (EP459Y clone, Abcam) directed against a cytoplasmic epitope within CD20 molecule or isotypic control in 1% BSA-PBS. After washes in PBS, Abs were revealed using Alexa Fluor 488-conjugated goat anti-rabbit IgG Ab (Invitrogen) for 30 min at 4 °C. After washing twice in PBS, cells were suspended in PBS and analysed by flow cytometry.

Real-time quantitative PCR analysis of *MS4A1* expression

Total RNA was isolated using the QIAzol Lysis Reagent from Qiagen, and 2 µg of total RNA was used as a template for complementary DNA (cDNA) synthesis using the High-Capacity cDNA Reverse Transcription Kit (Applied Biosystems), according to the manufacturer's instructions. Experiments were performed in triplicate with TaqMan® Fast Universal PCR Master Mix (Applied Biosystem Thermo Fisher Scientific) and membrane-spanning 4-domains A1 (*MS4A1; CD20*) specific primers and probe, or 18S TaqMan® Gene Expression Assays (Primer/Probe Set). Amplification of cDNA was measured using a StepOnePlusTM Real-Time PCR System (Applied Biosystem). Quantitation of results was determined using the delta delta CT method. *MS4A1* mRNA expression in DLBCL cells was normalised to 18S RNA levels (delta CT) and then expressed relative to culture condition control (delta delta CT). Primers used for *MS4A1:* forward primer 5′-ATGTCTTCACTGGTGGGCC-3′ and reverse primer 5′-TAATCTGGACAGCCCCCAA-3′ and sequence of the *MS4A1* TaqMan® probe: 5′-CACGCAAAGCTTCTTCATGAGGGAATCT-3′.

EV separation, analysis and quantification

sEV preparation from DLBCL cell culture medium. EVs were harvested from 72 h supernatants of DLBCL cell lines cultured in RPMI-1640 with 10% EV-depleted FBS by differential centrifugation and ultracentrifugation, according to standard protocols [28] and update of the MISEV2014 guidelines [29]. Briefly, supernatants were sequentially centrifuged (4 °C) at $300 \times g$ for 10 min, at $2000 \times g$ for 10 min and at $10{,}000 \times g$ for 30 min, followed by filtration (0.22 µm filter; Millipore). Then, sEVs were pelleted by ultracentrifugation at $120{,}000 \times g$ for 70 min and washed in PBS by a repeated $120{,}000 \times g$ centrifugation (SW28 rotor, Beckman Coulter). Supernatants were carefully removed and sEV pellets were suspended either in 50 µL of RIPA lysis buffer (when used for western blotting) or in 500 µL of PBS or enzyme-linked immunoassay (ELISA) sample buffer (when used for nanoparticle tracking analysis (NTA) analysis or CD20 ELISA, respectively), or in RPMI medium for in vitro or in vivo functional experiments.

Nanoparticle tracking analysis. Structural and quantitative analysis of EVs secreted by DLBCL cells was performed using the NanoSight NS300 instrument (Malvern Instruments Company), following the manufacturer's protocol. Mean particule sizes, modus and concentration of EVs were determined using the NTA 2.3 software in which five videos of 60 s were taken under controlled fluid flow with a pump speed set to 100. Plots represent the average value of the five recordings performed for each sample.

Electronic microscopy
Purified sEVs were captured using immunobeads coupled with anti-CD63 antibodies and analysed using transmission electron microscopy (TEM) at the Poitiers University (Service Anatomie et Cytologie Pathologiques CHU-La Milétrie).

Flow cytometry analysis of complement-dependent cell cytotoxicity (CDC)
Functional analysis of sEVs binding capacity to Rtx was evaluated by the rescue of DLBCL cell lines from Rtx-mediated CDC. Non-inactivated pooled normal human serum obtained from voluntary healthy donors was used as a complement source. Autologous or heterologous sEV preparations from 40×10^6 DLBCL cell supernatants were pre-incubated or not with 0.1 µg of Rtx in serum-free medium at 37 °C for 10 min. Then, fresh DLBCL cell cultures (10^6 cells/mL) were added, followed by the addition of human serum (20% vol/vol). After 30 min of incubation at 37 °C, cells were washed and resuspended in 500 µL of PBS. Cell death was analysed using propidium iodide (PI, 0.5 mg/mL) by flow cytometry (FACSCalibur, Becton Dickinson).

Western blotting analysis
Cell or sEV pellets were treated with RIPA buffer (Cell Signalling Technology) supplemented with protease and phosphatase inhibitors (Sigma). After centrifugation at $12{,}000 \times g$ for 20 min, the supernatant was collected. Twenty to 80 µg of proteins were separated by sodium dodecyl sulfate-polyacrylamide gel electrophoresis and then transferred to PVDF membrane (Bio-Rad). The primary Abs used were: mouse anti-human CD20 (Dako), anti-CD81 (Santa Cruz Biotechnology), anti-ALIX (Cell Signalling Technology) and anti-β-actin (Sigma-Aldrich); rabbit anti-CD63 (Abcam), anti-flotillin-1 and anti-flotillin-2 (Cell Signalling Technology) and anti-p-TrkB (Y817) (Abcam). Horseradish peroxidase (HRP)-conjugated secondary antibodies were from DakoCytomation. Blotted proteins were detected and quantified using the Immobilon Western Chemiluminescent HRP Substrate (Millipore) and a bioimaging system (GeneSnap; Syngene). Protein expression was quantified using ImageJ software (NIH). Alternatively, sEV preparations were first immunocaptured with magnetic Dynabeads® ProteinG (Invitrogen) conjugated with mouse IgG2a anti-human CD20 (Dako) according to the manufacturer's protocol. After overnight incubation with rotation at 4 °C, bead-bound sEV complexes were washed three times in PBS and finally resuspended in RIPA buffer with protease and phosphatase inhibitors for western blotting analysis.

Quantification of CD20 proteins on sEVs by ELISA
sEV preparations from DLBCL (produced by 40×10^6 cells) were resuspended in ELISA sample buffer, and CD20 level was quantified using CD20/MS4A1 (human) ELISA Kit (BioVision) according to the manufacturer's protocol. The limit of detection was 0.156 ng/mL.

In vivo xenografts
All animal studies were conducted in accordance with the guidelines established by the internal Institutional Animal Care and Use Committee (CREEAL No. 2-07-2012). Four-week-old SCID mice (CB17.SCID) were supplied by Janvier Labs (Le Genest-Saint-Isle, France). To analyse the in vivo function of sEV, we used a DLBCL xenograft model as previously reported [26, 30]. SCID mice were injected with 1×10^7 SUDHL4 cells subcutaneously. When tumours were established (~6 weeks after tumour cells inoculation), mice were randomly divided into different groups (six mice per group, control, treated with Rtx, treated with autologous or heterologous sEVs from control or 7,8-DHF cell cultures, treated with both Rtx and sEVs). Rtx (25 mg/kg) was administered intraperitoneally (i.p.) twice a week, alone or in combination with a contralateral i.p. injection of purified sEVs ($1{\times}10^7$ cell-derived sEV) from 72 h DLBCL cell cultures (SUDHL4) exposed or not to 7,8-DHF (500 nM). For control mice, treatment with vehicle alone was used and injections were realised with the same protocol as treated mice. Animals weighted ~20 g on the day of treatment. All animals were ear-tagged and monitored individually throughout the experiment. Tumour volume (cm^3) was estimated every 3 days during 2 weeks by measurements of the length (L), width (W) and height (H) of the tumour using the formula: volume $= L \times W \times H$. Mice were euthanised after 14 days of treatment by asphyxiation with CO_2, followed by cervical dislocation.

Statistical methods
Statistical significance between groups in the in vitro and xenograft studies was determined by a two-tailed Student's t test. $P < 0.05$ was considered statistically significant.

RESULTS
Characterisation of EV preparations from DLBCL cell cultures and analysis of CD20 expression
ABC- and GCB-DLBCL-derived EVs were isolated from cell culture supernatants (30×10^6 cells) by differential centrifugation. Characterisation of sEVs was performed using transmission electron microscopy and NTA (NanoSight). The mean size of EVs derived from the five tested DLBCL cell lines was 137 ± 6 nm with a modus mean of 111 ± 3 nm (Fig. 1a, b and Table 1a). Moreover, western blot analysis revealed the expression of CD63, flotillin-1/2 and CD81 proteins (Fig. 1c, as also shown in Fig. 2b for CD81) commonly used as sEV markers, including exosomes; indeed, the endosomal origin of some sEVs (exosomes) was also confirmed by the expression of MVB-derived protein (i.e. ALIX, Supplementary Fig. S1). These proteins were detected in sEV samples after 48 h of cell culture and were enriched after 72 h (Fig. 1c). Of note, as the level of flotillin-2 was higher than flotillin-1 in our samples, we have chosen flotillin-2 for the following experiments. Even if DLBCL-derived sEVs were very homogeneous in size, we observed some variations in the concentration of sEVs produced by each cell line (Table 1b). Indeed, the ABC cell line OCI-LY10 was the least productive cell line with a significantly lower EV concentration when compared to SUDHL6 and OCI-LY3. Furthermore, OCI-LY3 and, to a lesser extent, SUDHL6 are the most productive cell lines, with a significantly higher EV production than the other cell lines (OCI-LY3) or with OCI-LY3 and OCI-LY10 (SUDHL6). Moreover, our data strongly suggest no difference in cell capacity to produce sEVs according to the DLBCL subtype, as the highest productions were observed in GCB (i.e. SUDHL6) as well as in ABC (i.e. OCI-LY3) cell lines.

Among the DLBCL cell lines tested, CD20 membrane expression was heterogeneous and U2932 cells showed the lowest CD20 expression at the cell membrane and at the intracellular level (Fig. 2a, b). This was also confirmed by the lowest $CD20^+$ cell percentages (Table 2). As expected, western blot analysis showed that GCB- and ABC-derived sEVs carried CD20 (Fig. 2b). As shown in Fig. 2b, the levels of CD20, but also of CD81 and to a lesser extent flotillin-2, varied between DLBCL cell lines when total protein quantification was used to normalise our EV samples. Thus, we decided for the following experiments to use the same number of viable cells that produced sEVs for sample normalisation. CD20 expression of sEVs was also confirmed by enzyme-linked immunosorbent assay (ELISA) (Fig. 2c). Of note, sEVs from the U87-MG human glioblastoma cell line were used as negative controls in order to verify the specificity of CD20 detection (Fig. 2c). As shown by western blot analysis, CD20 level on sEVs from the U2932 cell line was below the detection threshold of the ELISA Kit used. Even though some high variability was found for CD20 level on OCI-LY3 sEV, our data obtained by ELISA were in good agreement with those obtained by western blot analysis of sEV lysates. Taken together, except for the OCI-LY3, these data showed that CD20 expression on sEVs produced by DLBCL cells reflects those on parental cells, as expected, notably at the membrane level. Indeed, OCI-LY10 and U2932 sEVs expressed the lowest CD20 level (especially for U2932, which was under the limit of detection) and, apart from OCI-LY3, SUDHL6 seemed to release sEVs with the highest CD20 level, as in their respective parental cells. Furthermore, these data suggest, for the first time, that the CD20 level on sEVs seems not to be in relation with the DLBCL subtype and thus aggressivity.

The TrkB agonist, 7,8-DHF, enhances CD20 level in DLBCL sEV
We have previously shown an autocrine BDNF/TrkB survival signalling axis in DLBCL [26]. To further explore the TrkB

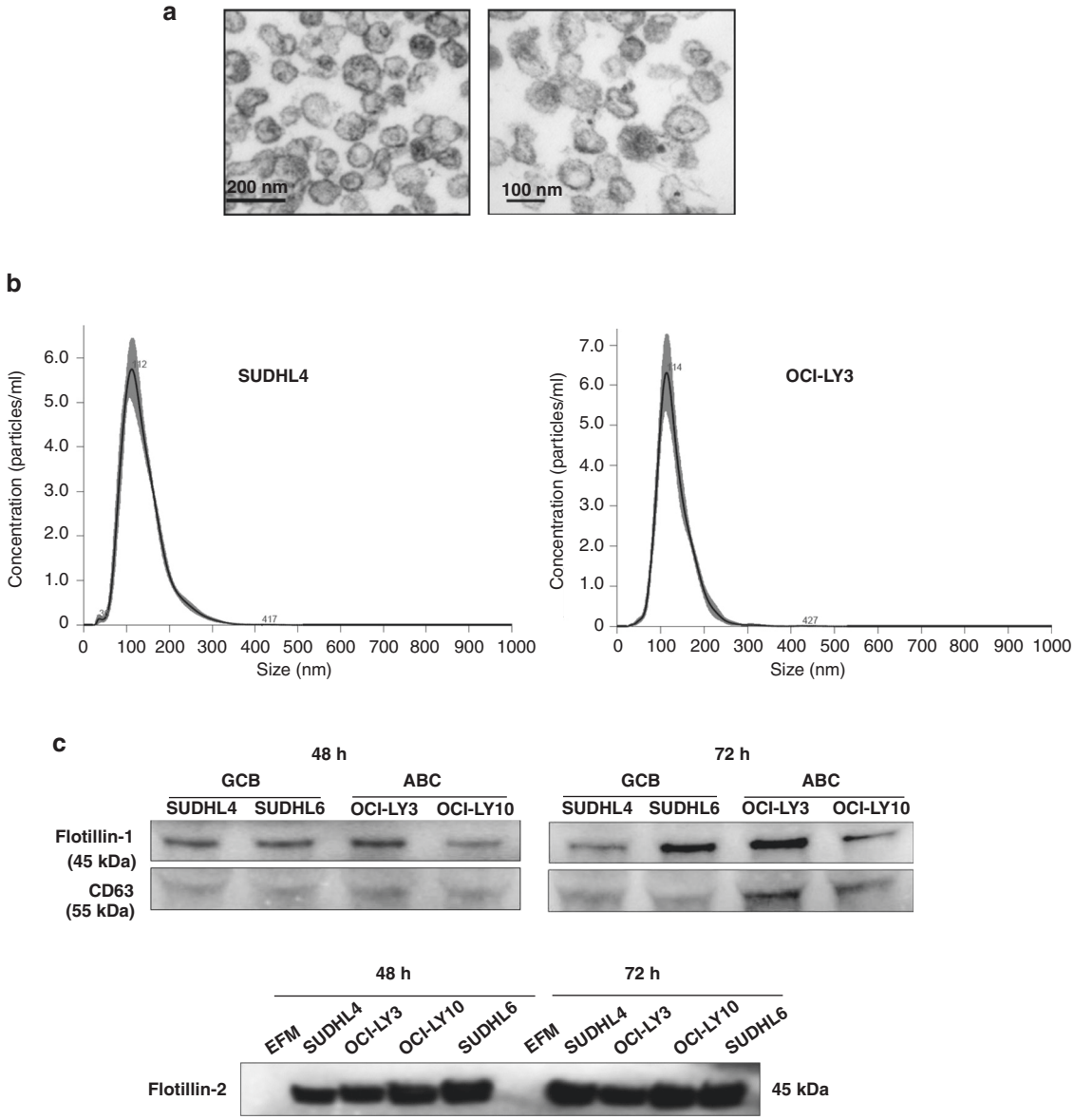

Fig. 1 Characterisation of small EVs produced by GCB and ABC-DLBCL cell lines. a Structural analysis of OCI-LY3-derived sEVs: micrographs from transmission electron microscopy (TEM) of immunocaptured EVs with anti-CD63-coupled immunobeads. **b** Nanosight tracking analysis (NTA) size distribution profile for representative EV preparations produced by DLBCL cell lines. Results are shown for SHDHL4 (GCB subtype) and OCI-LY3 (ABC subtype). Plots represent the mean value (black line) with standard error (red shaded area) of five recordings. **c** Representative western blot bands for analysis of small EV markers (i.e. flotillin-1 and -2; CD63) in total EV lysates from 48 and 72 h supernatants of DLBCL cell line cultures (10×10^6 cells). EFM EV-free medium used in the cell cultures.

mechanisms involved in DLBCL cells, we used a TrkB agonist (7,8-DHF) and we focused our study on EV production and CD20 expression. DLBCL cell lines were pre-exposed or not for 24 h to 7,8-DHF (500 nM) and then Rtx (1 µg/mL) was added or not in EV-free complete medium for an additional 48 h. Finally, sEVs were enriched from cell supernatants and analysed. 7,8-DHF-induced TrkB activation was confirmed, as previously reported [26], by enhanced phosphorylation (Y817) of the receptor (Fig. 3a). sEV production was analysed by NTA in GCB and ABC-DLBCL cell lines as shown for SUDHL4 and OCI-LY3 in Table 3. Particle size and distribution of EV, which confirmed to be consistently in the reported range of small EVs including exosomes, were not significantly modified by 7,8-DHF treatment; however, there was a trend towards an increase, even though not significant, in EV concentrations produced by SUDHL4 and OCI-LY3 cell cultures incubated with TrkB agonist as compared to culture controls (Table 3).

CD20 expression was first analysed at the protein (72 h; Fig. 3b, c) and transcriptional (*MS4A1* mRNA) (48 h; Fig. 3d) levels in Rtx and or 7,8-DHF-treated SUDHL4 cells. Our data confirmed the Rtx-induced decrease of CD20 cellular level, as shown for SUDHL4 cells in Fig. 3b by flow cytometry analysis. For this study, to prevent the blockage of the CD20 extracellular domain by Rtx, we used an anti-CD20 that recognises an epitope in the cytoplasmic domain of CD20 antigen, after cell permeabilization. Moreover, Rtx cell exposure seemed to affect notably the hypophosphorylated form of CD20 (western blotting analysis; Fig. 3c). Of note, the decrease of CD20 protein expression was not explained by a lower *MS4A1* mRNA level (Fig. 3d). When cells were incubated with the TrkB agonist, DHF, no modification of the CD20 level was observed at the protein (Fig. 3b, c) and mRNA levels (Fig. 3d). These results were also found with the physiological ligand (i.e. recombinant human BDNF 100 ng/mL), as shown in Fig. 3c, d. These same

Table 1. Morphological characterisation and quantification of EV preparations from 72 h culture supernatants of GCB (SUDHL4/6) and ABC (OCI-LY3/10, U2932) DLBCL cell lines. (a) Mean particle size, modus[a] and (b) concentration of EVs released by 30×10^6 cells[a].

(a)

Subtype	DLBCL cell line	Particule size (nm) (means ± SE)	Modus (nm)
GCB	SUDHL4	130 ± 10	106 ± 15
	SUDHL6	143 ± 12	116 ± 11
ABC	OCI-LY3	141 ± 14	112 ± 7
	OCI-LY10	141 ± 15	111 ± 6
	U2936	132 ± 26	111 ± 18

(b)

Concentration ($\times 10^8$ particles/mL)	SUDHL4	SUDHL6	OCI-LY3	OCI-LY10	U2932
SUDHL4	4 ± 2				
SUDHL6	$p = 0.15$	6 ± 3			
OCI-LY3	$\mathbf{p = 0.03}$	$\mathbf{p = 0.05}$	20 ± 15		
OCI-LY10	$p = 0.10$	$\mathbf{p = 0.02}$	$\mathbf{p = 0.03}$	2 ± 1	
U2932	$p = 0.72$	$p = 0.12$	$\mathbf{p = 0.03}$	$p = 0.31$	3 ± 2

Bold value indicate statistical significance $p \leqslant 0.05$.
[a]They were quantified using the NanoSight Tracking Analysis system after small EV enrichment by ultracentrifugation as described in 'Materials and methods'. Results are expressed as means ± SD of at least five independent experiments. The corresponding statistical comparisons of EV production between cell lines are done (p value, t test).

results were also found with the ABC cell line, OCI-LY3 (data not shown).

CD20 expression was further analysed by western blot on sEVs derived from supernatants of DLBCL cell cultures. Flotillin-2 and/or CD81 in EV lysates were used as sEV-associated proteins (Fig. 4) and as control of EV yields when total sEV lysates were loaded. Our data suggested an increase in CD20 level in total sEV lysates from DHF-treated SUDHL4 cell cultures (Fig. 4a), in contrast to the decrease observed after Rtx exposure (Supplementary Fig. S2). Of note, western blot analysis of flotillin-2 and/or CD81 levels in total sEV lysates showed that part of this DHF-enhanced CD20 expression could be related to an increase in the sEV number, as suggesting data from NTA analysis. However, the quantification analysis of five experiments revealed a significantly higher CD20 level normalised to the amount of CD81 in sEVs released by DHF-treated cells as compared to sEVs of the control culture. We confirmed this result by western blot analysis of immuno-captured sEVs as shown in Fig. 4b. Interestingly, enhanced CD20 level with or without a simultaneous increase of CD81 was also observed after TrkB stimulation with the physiological ligand, BDNF, and in sEVs of other GCB (i.e. SUDHL6) and ABC (i.e. OCI-LY3, OCI-LY10) cell lines (Fig. 4c and Supplementary Fig. S1). Moreover, in contrast, to control culture conditions (Fig. 4a), we found some co-isolated contaminants of proteins localised in other compartments like nucleus (i.e. PARP) and mitochondria (i.e. TOM20) when sEVs were isolated from 7,8-DHF-treated cell supernatants. Collectively, these data suggest that TrkB agonist signalling determines higher CD20 in sEVs and/or release of sEVs that contain sEVs like exosomes but also other subtypes of EVs.

DLBCL cells are differentially protected by autologous sEVs from Rtx cytotoxicity and the effect of sEVs from TrkB agonist-treated cultures

Previous data showed that sEVs released from aggressive B-lymphoma cells act as decoy targets upon Rtx exposure, allowing cells to escape from humoral immunotherapy [19]. With the aim to further explore this protective effect in vivo and also with sEVs from TrkB-activated cell cultures, we first evaluated in vitro the capacity of our sEV preparations to influence the sensitivity of DLBCL cell to Rtx, and notably to the complement-dependent Rtx cytotoxicity (CDC). We have chosen to focus our analyses on SHDHL4 cells as we used SUDHL4 xenograft-bearing mice for the in vivo study.

Results showed (Fig. 5a) that when autologous sEVs are added to cell cultures, sensitive DLBCL cells (i.e. SUDHL4, SUDHL6 and OCI-LY10) became more resistant to Rtx-mediated CDC with a strong decrease in dead cell percentages when compared to Rtx alone. Of note, cell viability was not modified by co-culture with sEVs alone for all studied cell lines. Interestingly, autologous sEVs induced total Rtx escape of SUDHL6 cells, as CDC with sEVs from SUDHL6 was no longer significantly different from the CDC control (Fig. 5a). Of note, a positive correlation was observed between CD20 membrane expression (MFI) of each cell line and sEV-mediated CDC protection (correlation coefficient = 0.92; $R^2 = 0.85$). These data show that sEV-mediated escape from CDC is linked to the cell sensitivity (i.e. membrane CD20 level) to Rtx. In the ABC-DLBCL subtype cell line, OCI-LY3, known to be more resistant, Rtx (0.1 µg/mL) exposure did not induce CDC, which could be explained by the lower CD20 membrane expression as compared to responsive cell lines (Table 2). Furthermore, viability was not changed when cells were exposed to sEVs alone (Fig. 5a). To further investigate the role of CD20 level in the protective effect of sEVs from the Rtx-induced CDC, we analysed the influence of heterologous sEVs with different levels of CD20 on the CDC sensitivity of SUDHL4 cells. Our results showed (Fig. 5b) that the CDC escape realised by sEVs is dependent on their CD20 level, with a strong escape observed for sEVs with high CD20 expression (SUDHL6, OCI-LY3 and SUDHL4) and a low or no escape for sEVs with lower (SUDHL10) or negative (U2932) CD20 expression. Interestingly, the protective effect of sEVs from SUDHL6 was significantly higher than those of sEVs from the other DLBCI cell lines. These data with recent preliminary results obtained by flow cytometry (Supplementary Fig. S3) confirm the functionality of all SUDHL-derived sEVs tested, likely by exercising a decoy function against anti-CD20 antibodies.

Finally, as treatment with 7,8-DHF seemed to enhance sEV CD20 expression, we explored the in vitro capacity of autologous sEVs isolated from DHF-treated SUDHL4 cell cultures to enhance protection against Rtx-mediated CDC. Indeed, our results (Fig. 5c) showed that, even if the effect was low, CDC escape was higher

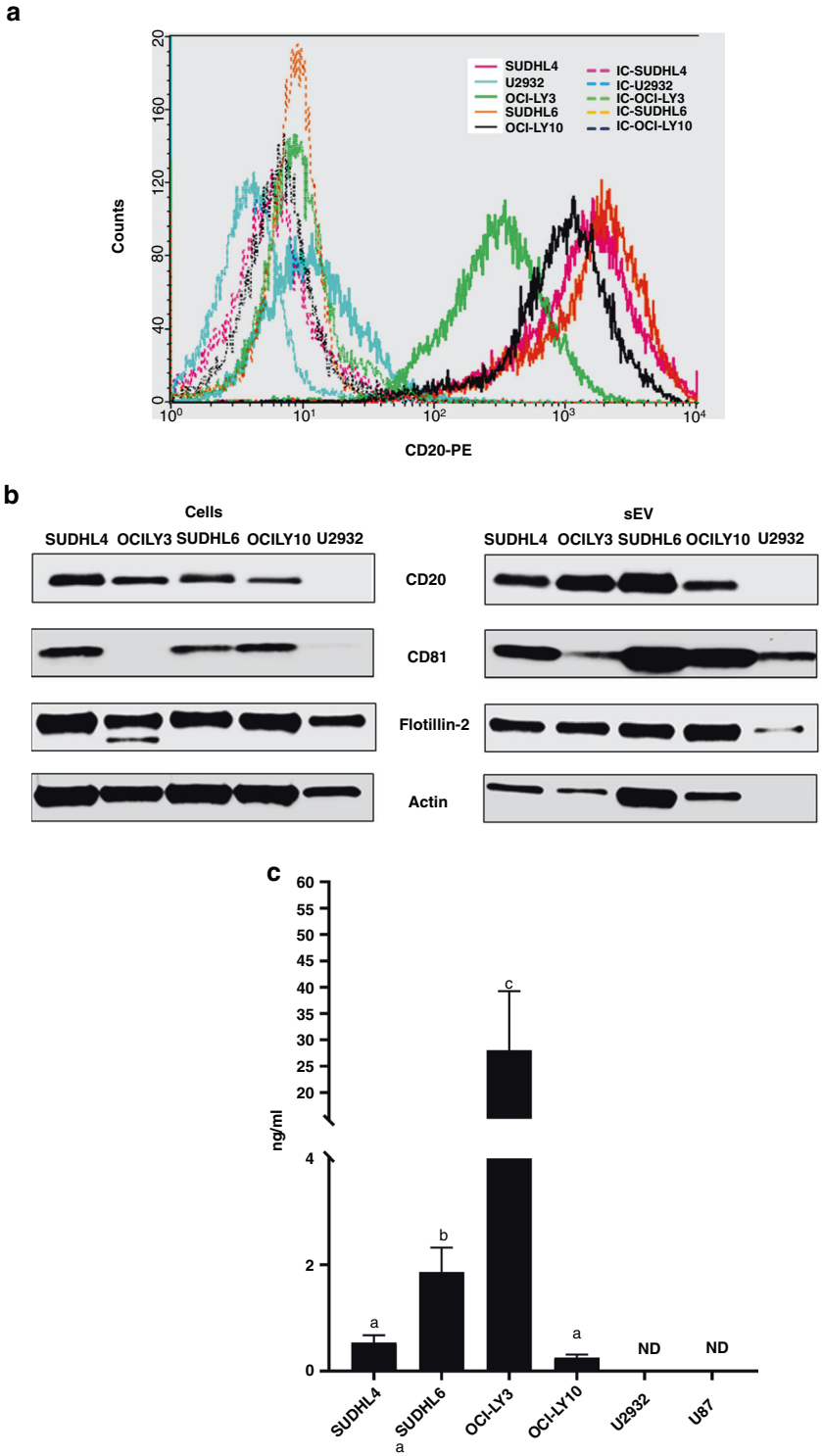

Fig. 2 CD20 expression in DLBCL cell lines and small EV. a CD20 surface expression was determined using anti-CD20-PE by flow cytometry in GCB (SUDHL4 and SUDHL6) and ABC (OCI-LY3, OCI-LY10 and U2932) DLBCL cell lines. Representative histograms are shown: solid outline histograms indicate the expression of CD20 in DLBCL cells; dashed lines are the fluorescence intensity of cells labelled with isotype control mAb. **b** Western blot analysis of CD20 and small EV marker proteins (CD81, flotillin-2) in EV lysates as compared to cell lysates (72 h—10 µg of protein/well). CD20 expression was not detected in U2932 cell lysates using 10 µg of protein, but was found with 20 µg only in cells (data not shown). Actin is shown as the loading control. Data are representative of at least three independent experiments. **c** Levels of CD20 on small EVs produced by 40×10^6 DLBCL cells as assayed by ELISA; results (ng/mL) are expressed as means ± SEM of four (SUDHL4, SUDHL6, OCI-LY3 and OCI-LY10) or three (U2932 and U87) independent experiments. ND not detected. Data with a statistically significant difference are labelled with different letters (a, b, c = $p < 0.05$, *t* test).

Table 2. Flow cytometry analysis of membrane CD20 expression on GCB (SUDHL4 and SUDHL6) and ABC (OCI-LY3, OCI-LY10 and U2932) DLBCL cell lines.

CD20 cell surface expression	SUDHL4	SUDHL6	OCI-LY3	OCI-LY10	U2932
MFI	1824 ± 50	1989 ± 18	389 ± 1	1195 ± 21	23 ± 5
Positivity (%)	99 ± 0	99 ± 0	98 ± 0	99 ± 0	76 ± 2

Membrane CD20 expression was analysed by flow cytometry after anti-CD20-PE staining of DLBCL cells. Data are the means of three experiments ± SD.
MFI mean fluorescence intensity of CD20 staining.

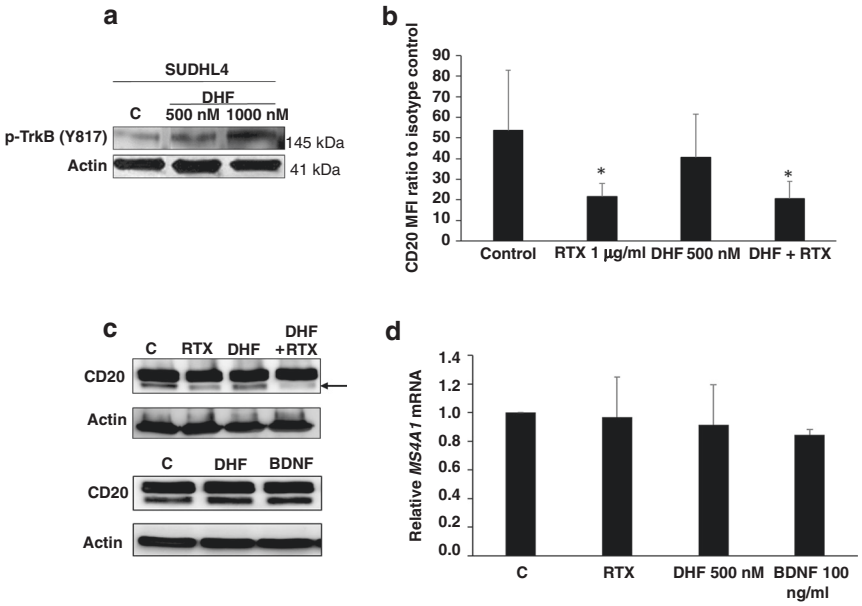

Fig. 3 Effect of TrkB activation on CD20 expression in DLBCL cells. a TrkB activation by 7, 8-dihydroxyflavone (7,8-DHF, 500 and 1000 nM) was confirmed using anti-phospho-TrkB (Y817) by western blot analysis in 48 h SUDHL4 cell lysates (80 µg of protein/well) as compared to control lysates (C, DMSO control). **b** Cellular CD20 level was analysed by flow cytometry after permeabilization of SUDHL4 cells incubated with or without rituximab (1 µg/mL) and/or 7,8-DHF (500 nM). Data from five independent experiments are expressed as means ± SD of the ratio of mean fluorescence intensity (MFI) of stained cells to MFI of respective isotype control. Statistical significance between groups vs control was assessed using a paired two-tailed *t* test, $*p < 0.05$. **c** Representative western blot bands from at least two independent experiments for CD20 intracellular expression of SUDHL4 cells exposed or not (C, control) to rituximab (1 µg/mL) and/or 7,8-DHF (500 nM). Alternatively, the physiologic TrkB ligand, BDNF, was used (rhBDNF 100 ng/mL) (20 µg of protein/well). The hypophosphorylated form of CD20 is indicated by an arrow. Actin is shown as a loading control. **d** Relative quantification by qRT-PCR analysis of *MS4A1* mRNA levels in SUDHL4 cell cultures. *MS4A1* mRNA was normalised to 18S RNA levels and then expressed relative to culture condition control. Histograms represent means ± SD of four or two (for BDNF) independent experiments.

with sEV preparations from DHF-treated cell cultures (Rtx + sEV4 DHF) than that of the control culture (Rtx + sEV4). Of note, we also observed the same trend with sEVs from OCI-LY10 cell cultures on autologous cell protection from Rtx-mediated CDC (data not shown). However, no effect was observed for sEVs from DHF-treated SUDHL6 cell supernatants (data not shown). This result could be explained by the strong protection already done by SUDHL6-derived sEVs from control cultures (Fig. 5a).

sEVs allow in vivo tumour escape from Rtx treatment in a DLBCL xenograft mouse model

In order to confirm our data in vivo, we used a GCB-DLBCL xenograft murine model as previously reported [26, 30, 31], in which SCID mice were subcutaneously inoculated with SUDHL4 cells. After 6 weeks, tumour-bearing mice were i.p. treated with Rtx (25 mg/kg) or PBS solution (control mice), in association or not with autologous sEVs purified from 10×10^6 SUDHL4 cell cultures in the presence or not with 7,8-DHF (500 nM). Moreover, the in vivo capacity of heterologous OCI-LY3-derived sEVs to protect SUDHL4 tumours from Rtx cytotoxicity was also evaluated.

Tumour growth in mice treated only with SUDHL4- or OCI-LY3-derived sEVs purified from control cultures (sEV4 or sEV3, respectively) was not significantly different from those of PBS-treated control mice (Fig. 6a, n.s.). Our data showed that, when associated with Rtx treatment, sEV preparations (sEV4 or sEV3 + Rtx) induced a significant increase of tumour growth, compared to mice injected with Rtx alone; this escape from Rtx was stronger with the heterologous OCI-LY3-derived sEV, confirming our in vitro findings. Indeed, tumour volumes were no longer significantly different from those of control mice (Fig. 6a). Interestingly, enhanced protection was observed when sEVs were purified from TrkB agonist-treated cell cultures (i.e. sEV4 DHF + Rtx in Fig. 6b) and tumour growth was significantly higher ($p < 0.05$) compared to mice receiving sEVs purified from control cultures (i.e. sEV4 + Rtx). Of note, no significant effect was observed with sEVs from DHF cell cultures alone (i.e. sEV4 DHF). To the best of our knowledge, these data show, for the first time, the in vivo capacity of DLBCL-derived sEVs to protect tumours from Rtx treatment in a DLBCL xenograft model, which could also be enhanced using sEVs produced by cells with TrkB activation.

DISCUSSION

Increasing evidences support an important role for exosomes in haematological malignancies including DLBCL development and

Table 3. Effect of the TrkB agonist (7,8-DHF) on sEV production by DLBCL cells.

	SUDHL4			OCI-LY3		
	Control	DHF (500 nm)	*P* value	Control	DHF (500 nm)	*P* value
Particle size (nm) (means ± SE)	132 ± 9	133 ± 10	0.87	143 ± 14	142 ± 19	0.82
Modus (nm)	108 ± 14	105 ± 9	0.64	114 ± 7	114 ± 5	0.94
Concentration ($\times 10^8$ particles/mL)	3 ± 1	6 ± 7	0.33	25 ± 29	45 ± 53	0.08

Mean particle size, modus and concentration of sEVs were quantified using the NanoSight Tracking Analysis system after sEV enrichment by ultracentrifugation as described in 'Materials and methods'. Results are expressed as means ± SD of eight independent experiments. *P* values of paired-samples *t* test are done.

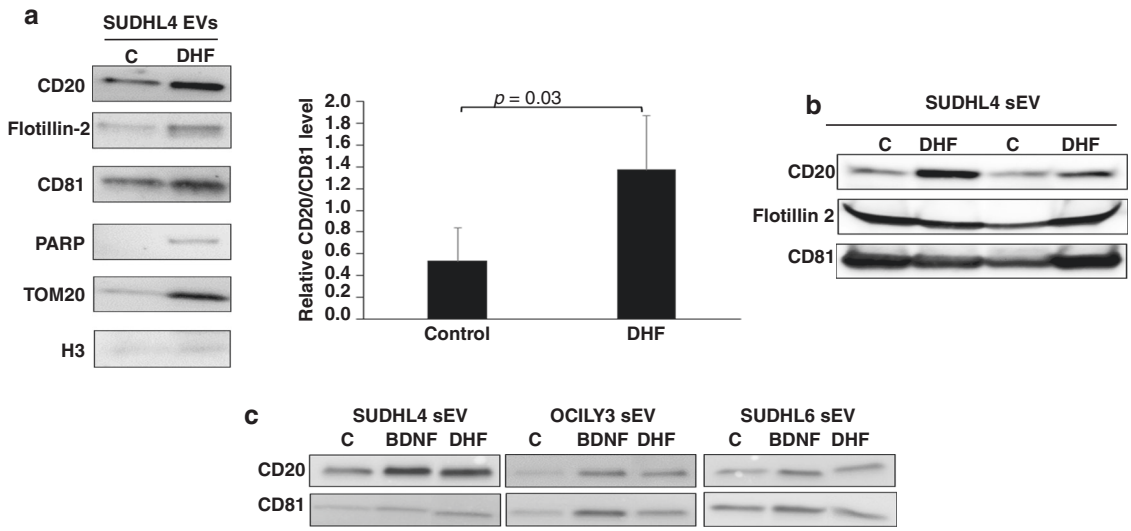

Fig. 4 TrkB activation enhances CD20 expression on DLBCL-derived small EV. a Western blot analysis of proteins in sEV lysates from 72 h supernatants of SUDHL4 cell cultures in the presence or not (C, control) of 7,8-DHF (500 nM). Total sEV lysates produced by 40×10^6 cells were used for each culture condition. Expression of CD20, sEV markers (flotillin-2 and CD81) and also (in two independent experiments) mitochondrial (TOM20) and nuclear (PARP and H3) markers were assessed. Histograms show quantification by densitometry of CD20 expression normalised to CD81 level of five independent experiments. **b** Alternatively, anti-CD20 immunocaptured EVs were used before western blot analysis of total small EV lysates produced by 20×10^6 cells. **c** Enhanced CD20 expression with or not CD81 increase was also found in total sEV lysates from SUDHL6 and OCI-LY3 cells, as for SUDHL4, after TrkB activation by DHF but also the physiologic ligand, BDNF (rhBDNF 100 ng/mL). Images are representative of two independent experiments.

progression [32, 33]. However, the mechanisms of CD20 regulation at the exosomal level needed to be clarified for the different DLBCL cell subtypes. In the present study, we realised a comparative analysis of sEV production by GCB and ABC-DLBCL cell lines and evaluated their CD20 level. NTA and western blot data demonstrated sEVs in our preparations, which probably included exosomes. Multiple normalisation strategies are found in published studies (particle counts, total amount of biomolecules like proteins, or the number of secreting cells for in vitro studies) and no clear recommendation can be made on which normalisation is best [29]. In the present work, as sEV productions by the studied DLBCL cell lines were low and probably heterogeneous, we have used the same viable cell number rather than total protein quantification to normalise our sEV samples.

As reported for membrane CD20 level among tumour B cell lines, or in patients [34, 35], CD20 expression of sEVs was variable, with a higher level for sEVs derived from cell lines expressing high membrane CD20 levels (i.e. SUDHL6). As expected, CD20 expression was mostly undetectable in sEV lysates produced by U2932 cells that were also $CD20^{low}$, and CD20 was not detected at the cellular (data not shown) and sEV levels in a $CD20^-$ glioblastoma cell line. The differential CD20 expression of sEVs obtained by the western blot analysis was confirmed by ELISA, and, except for the OCI-LY3 cell line, these levels are in good agreement with the CD20 level of parental cells. Moreover, the lower CD20 level of OCI-LY10 and U2932 sEVs observed by western blot and ELISA was also confirmed by preliminary results obtained by flow cytometry analysis of the binding capacity of sEVs derived from DLBCL cell lines to Rtx (Supplementary Fig. S3). The Capture of Rtx was the lowest for sEVs from U2932 and to a lesser extent with sEVs from OCI-LY10. Collectively and by different approaches, we show in the present study that the CD20 level on sEVs reflects those of parental cells, except for OCI-LY3; indeed, the OCI-LY3 cell line forms cellular aggregates that were difficult to separate in the analyses, which may have interfered with some results. Our analysis suggests no significant difference according to the DLBCL subtype, even if we have to confirm this with additional cell lines as well as in sEVs from patients. As expected, we confirmed in vitro the functional capacity of autologous and heterologous sEVs to protect cells from Rtx-mediated CDC [19, 36]. CDC activity of Rtx has been shown to be dependent on CD20 expression level [37], which could explain the CDC resistance of OCI-LY3 in this study. Interestingly, our data revealed stronger protection in the autologous model (i.e. SUDHL6 sEVs vs SUDHL6 cells) or heterologous model (i.e. OCI-LY3 sEVs and SUDHL6 sEVs vs SUDHL4 cells) with sEVs that likely express higher CD20 levels and/or are highly concentrated in cell culture supernatants. Indeed, NTA data showed that sEV production varies significantly between some of the DLBCL cell lines, which was also suggested by western blot analysis. For SUDHL6, OCI-LY10 and U2932 cells, as no significant differences were shown with SUDHL4 sEV production by NTA (Table 1b), the

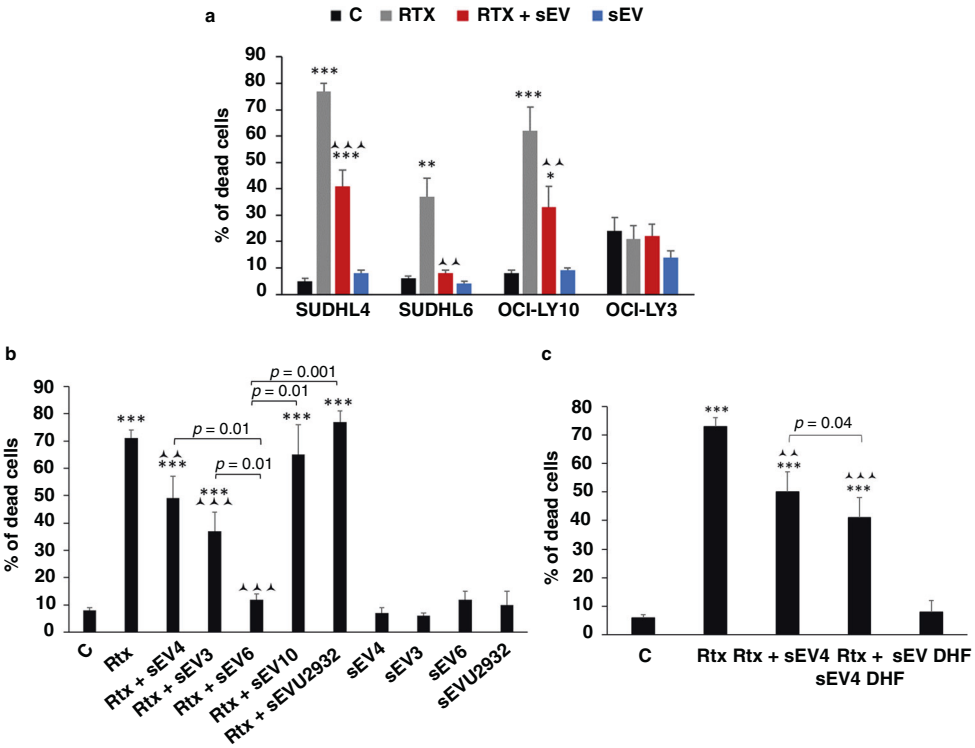

Fig. 5 In vitro analysis of the differential capacity of small EVs in protecting DLBCL cells from rituximab cytotoxicity and the effect of TrkB stimulation. a GCB (SUDHL4 and SUDHL6) and ABC (OCI-LY3 and OCI-LY10) DLBCL cell lines were cultured in the presence or not (C, control) of autologous small EV samples (sEVs) isolated from 40×10^6 cell supernatants, or/and rituximab (Rtx, 0.1 µg/mL). Rituximab-mediated complement-dependent cytotoxicity (CDC) was analysed by flow cytometry after 30 min in the presence of human serum. Dead cell (propidium iodide positive cells) percentages are shown and histograms represent means ± SEM of at least seven (SUDHL4/6 and OCI-LY10) and 4 (OCI-LY3) independent experiments. *,**, ***$P < 0.05$, 0.01 or 0.001 vs control; ⅄, ⅄ ⅄, ⅄ ⅄ ⅄: $p < 0.01$ or 0.001 vs RTX. **b** Alternatively, heterologous sEVs (derived from OCI-LY3, SUDHL6, OCI-LY10 and U2932: sEV3, sEV6, sEV10 and sEVU2932, respectively) were compared to autologous sEV4 in protecting SUDHL4 cells from rituximab CDC. Histograms represent means ± SEM of dead cell percentages from at least seven independent experiments. **c** Finally, autologous small EVs derived from SUDHL4 cultured with the TrkB agonist, 7,8-DHF (Rtx + sEV4 DHF) or not (Rtx + sEV4), were also evaluated for their capacity to modify SUDHL4 CDC susceptibility. Histograms represent means ± SEM of dead cell percentages from nine independent experiments.

higher (SUDHL6) or lower (OCI-LY10 and U2932) protection vs sEVs from SUDHL4 can be attributed to the higher or lower CD20 level of sEVs, respectively; for OCI-LY3, as this cell line was shown to produce a larger number of sEVs than other cell lines, the higher protection could also reflect higher sEV concentration.

We have previously shown that autocrine BDNF/TrkB survival pathways may affect Rtx efficacy in DLBCL [26]. Herein, we report for the first time in vitro and in vivo evidence for a TrkB role in cell escape from Rtx treatment that could involve sEV production and their CD20 expression. 7,8-DHF is a member of the flavonoid family that has been identified as the first small-molecule compound that crosses the blood–brain barrier, binds with high affinity and specificity to the BDNF receptor, TrkB, and activates its down-stream signalling cascade [27]. In the present work, we used 7,8-DHF to mimic the BDNF effect in DLBCL cells that we proved by enhanced phosphorylation of TrkB. Erk and Akt signalling pathways, involved in TrkB signalling [38], have also been described to control the up-regulated expression of CD20 on human tumour B cells [39, 40]. Thus, we evaluated the role of TrkB activation on the regulation of CD20 expression. We first analysed CD20 membrane and intracellular levels in DLBCL cells exposed to the TrkB agonist, 7,8-DHF, associated or not to Rtx. We confirmed, in the SUDHL4 cell, the previously reported down-regulation of CD20 level after Rtx exposure [10, 35]. However, we show that this effect was not associated with reduced mRNA *MS4A1* levels suggesting, as previously described, the complexity of mechanisms involved in Rtx-induced down-regulation of membrane CD20 [37]. As concerning sEVs released by DLBCL cell lines, we observed a decrease of CD20 expression after Rtx exposure (Supplementary Fig. S1); this result, reported here for the first time to our knowledge, strongly suggests that this variation in CD20 level reflects the down-regulation of the membrane CD20 level observed in parental cells. Interestingly, we found in sEV lysates, derived from DLBCL cell cultures, a higher expression of CD20 after 7,8-DHF exposure, which was not explained by an overall increase in cellular CD20 level neither in *MS4A1* mRNA. The higher CD20 expression on sEVs after TrkB activation was found in all tested DLBCL cell lines and was observed with the natural ligand of TrkB, BDNF. Of note, increased expression of CD20 in sEV lysates was often associated with an increase in sEV marker expression (i.e. CD81 or flotillin-2), suggesting that this effect could be due, at least partly, to an increase in sEV production. This hypothesis is supported by the NTA analysis of sEV preparations that were purified from DLBCL cell cultures after 7,8-DHF treatment as compared to control. However, we could not find any significant differences between our groups likely due to the high variability of sEV concentrations produced by each cell culture. Our previously reported data in DLBCL cell lines and biopsies samples from patients revealed the expression of full-length (TrkB.FL) and truncated (TrkB.T1) forms of BDNF high-affinity receptor, and $p75^{NTR}$, the low-affinity NT receptor [26]. Furthermore, we showed evidence for a pro-survival role of endogenous BDNF/TrkB/$p75^{NTR}$ axis in DLBCL cells that could be involved in aggressive phenotypes. Interestingly, in neurons BDNF/TrkB.FL/$p75^{NTR}$ signalling was demonstrated to induce internalisation and accumulation of $p75^{NTR}$, which had escaped the lysosomal route in $CD63^+$ MVBs for exosome release [41, 42]. Of note, $p75^{NTR}$ was

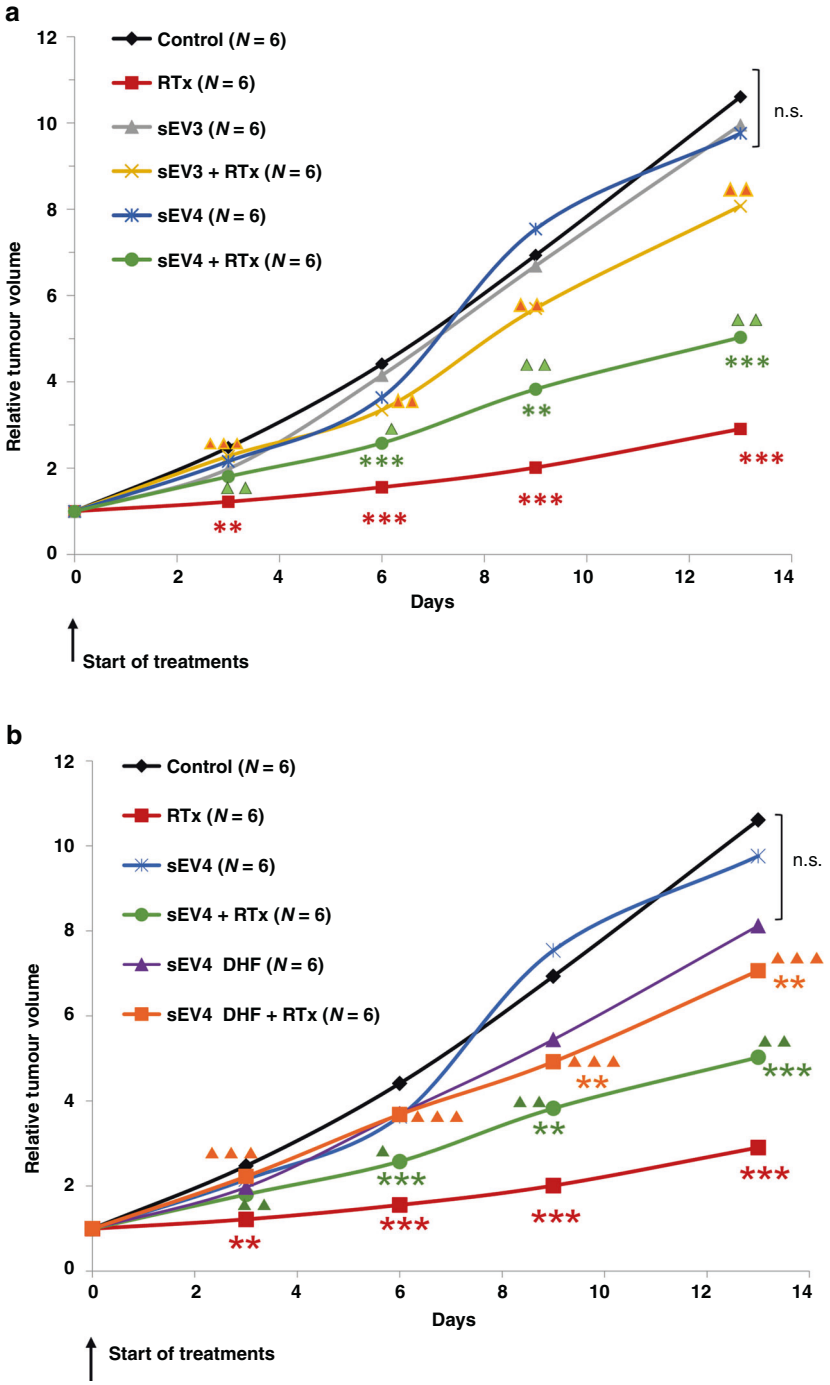

Fig. 6 Autologous and heterologous small EVs allow in vivo rituximab escape of tumour in a DLBCL xenograft model that is enhanced with EVs from Trk-stimulated cells. a SCID mice bearing tumours from SUDHL4 cells were injected i.p. twice a week, with or without (control) rituximab (Rtx, 25 mg/mL) alone or in combination with autologous (sEV4 + Rtx) or heterologous small EVs (sEV3 + Rtx) enriched from 72 h cell cultures (1×10^7 cells). Injection of only small EV samples (sEV3 and sEV4) was also realised. **b** Alternatively, mice were injected with Rtx in combination with autologous sEVs derived from SUDHL4 supernatants of cultures exposed to 500 nM of 7,8-DHF (sEV4 DHF + Rtx) or not (sEV4 + Rtx), as compared to mice injected with sEVs alone (sEV4 and sEV4 DHF). Tumour volumes (cm^3) were estimated during 2 weeks. Means of tumour volumes relative to day 0 obtained for six mice per group are shown, and SDs are not indicated for a better reading of the figure. **,***$p < 0.01$ or 0.001, respectively, vs control mice and ▲, ▲▲, ▲▲▲$p < 0.05$, 0.01 or 0.001, respectively, vs Rtx-treated mice. n.s. Not significant.

previously found in small EVs released by DLBCL cell lines (personal data). Therefore, even if we cannot exclude medium/large EVs in our preparations, we suggest that, as in neurons, BDNF/TrkB.FL/$p75^{NTR}$ signalling in DLBCL cells may increase internalisation and post-endocytic trafficking of membrane receptors as $p75^{NTR}$ favouring MVBs specialised for exosome release.

Results from our in vitro studies indicated higher CD20 levels in sEVs after TrkB activation, suggesting a potential effect in cell escape from Rtx-induced CDC. To assess this possibility in vivo, we used xenografts of SUDHL4 cells in SCID mice and evaluated the role of autologous sEVs purified from supernatants of SUDHL4 cell cultures treated or not with 500 nM of 7, 8-DHF. First, we

confirm in vivo, for the first time to our knowledge, in a DLBCL xenograft mice model, the capacity of autologous sEVs to protect DLBCL tumours from Rtx cytotoxicity. Moreover, data are consistent with in vitro results showing stronger protection with heterologous OCI-LY3-derived sEV, probably by exercising a higher decoy function against Rtx. Interestingly, we proved that this protection was significantly higher when sEVs were derived from SUDHL4 cells exposed to the TrkB agonist. Even though we proposed that an increase in CD20 expression of sEVs and/or sEV release is involved in this higher cell escape, we cannot exclude other EV components as a complement or complement regulatory proteins that have been also reported in sEVs from DLBCL [19]. Moreover, in vivo, sEVs can influence tumour microenvironment or inhibit target cells as NK cells by carrying genetic information notably microRNAs [43]. Indeed, further experiments are required to understand the in vivo mechanisms as well as TrkB-mediated regulation of CD20 levels in sEVs of DLBCL.

In conclusion, present data provide comparative quantitative and qualitative (i.e. CD20 levels) informations on sEVs released by GCB and ABC-DLBCL cell lines. Furthermore, they report in vivo (xenograft model) the capacity of autologous and heterologous sEVs to protect tumours from immunotherapy, which could be influenced and enhanced by culture conditions. Notably, we showed that autocrine/paracrine survival loops realised by BDNF/TrkB axis, which we previously reported in DLBCL, also target sEV release enhancing protection to Rtx. Finally, beyond their role in exercising a decoy function against Rtx, our results suggest that peripheral sEVs from patients, by providing indirect information on the CD20 phenotype of parental cells, could serve as a "liquid biopsy" in DLBCL disease monitoring.

DATA AVAILABILITY

All data presented within the article and its Supplementary information file are available upon request from the corresponding author.

REFERENCES

1. Alizadeh AA, Eisen MB, Davis RE, Ma C, Lossos IS, Rosenwald A, et al. Distinct types of diffuse large B-cell lymphoma identified by gene expression profiling. Nature. 2000;403:503–11.
2. Wright G, Tan B, Rosenwald A, Hurt EH, Wiestner A, Staudt LM. A gene expression-based method to diagnose clinically distinct subgroups of diffuse large B cell lymphoma. Proc Natl Acad Sci USA. 2003;100:9991–6.
3. Lenz G, Staudt LM. Aggressive lymphomas. N. Engl J Med. 2010;362:1417–29.
4. Coiffier B. Rituximab therapy in malignant lymphoma. Oncogene. 2007;26:3603–13.
5. Rezvani AR, Maloney DG. Rituximab resistance. Best Pract Res Clin Haematol. 2011;24:203–16.
6. Li S, Young KH, Medeiros LJ. Diffuse large B-cell lymphoma. Pathology. 2018;50:74–87.
7. Suzuki Y, Yoshida T, Wang G, Togano T, Miyamoto S, Miyazaki K, et al. Association of CD20 levels with clinicopathological parameters and its prognostic significance for patients with DLBCL. Ann Hematol. 2012;91:997–1005.
8. Czuczman MS, Olejniczak S, Gowda A, Kotowski A, Binder A, Kaur H, et al. Acquirement of rituximab resistance in lymphoma cell lines is associated with both global CD20 gene and protein down-regulation regulated at the pre-transcriptional and posttranscriptional levels. Clin Cancer Res J Am Assoc Cancer Res. 2008;14:1561–70.
9. Hiraga J, Tomita A, Sugimoto T, Shimada K, Ito M, Nakamura S, et al. Down-regulation of CD20 expression in B-cell lymphoma cells after treatment with rituximab-containing combination chemotherapies: its prevalence and clinical significance. Blood. 2009;113:4885–93.
10. Miyoshi H, Arakawa F, Sato K, Kimura Y, Kiyasu J, Takeuchi M, et al. Comparison of CD20 expression in B-cell lymphoma between newly diagnosed, untreated cases and those after rituximab treatment. Cancer Sci. 2012;103:1567–73.
11. Colombo M, Raposo G, Théry C. Biogenesis, secretion, and intercellular interactions of exosomes and other extracellular vesicles. Annu Rev Cell Dev Biol. 2014;30:255–89.
12. Doyle LM, Wang MZ. Overview of extracellular vesicles, their origin, composition, purpose, and methods for exosome isolation and analysis. Cells. 2019;8:727.
13. Kharaziha P, Ceder S, Li Q, Panaretakis T. Tumor cell-derived exosomes: a message in a bottle. Bio Biophys Acta. 2012;1826:103–11.
14. Kahlert C, Kalluri R. Exosomes in tumor microenvironment influence cancer progression and metastasis. J Mol Med. 2013;91:431–7.
15. Yu S, Cao H, Shen B, Feng J. Tumor-derived exosomes in cancer progression and treatment failure. Oncotarget. 2015;6:37151–68.
16. Hannafon BN, Ding WQ. Intercellular communication by exosome-derived microRNAs in cancer. Int J Mol Sci. 2013;14:14240–69.
17. Zhang X, Yuan X, Shi H, Wu L, Qian H, Xu W. Exosomes in cancer: small particle, big player. J Hematol Oncol. 2015;8:83
18. Ruivo CF, Adem B, Silva M, Melo SA. The biology of cancer exosomes: insights and new perspectives. Cancer Res. 2017;77:6480–8.
19. Aung T, Chapuy B, Vogel D, Wenzel D, Oppermann M, Lahmann M, et al. Exosomal evasion of humoral immunotherapy in aggressive B-cell lymphoma modulated by ATP-binding cassette transporter A3. Proc Natl Acad Sci USA. 2011;108:15336–41.
20. Koch R, Aung T, Vogel D, Chapuy B, Wenzel D, Becker S, et al. Nuclear trapping through inhibition of exosomal export by indomethacin increases cytostatic efficacy of doxorubicin and pixantrone. Clin Cancer Res. 2016;22:395–404.
21. Rutherford SC, Fachel AA, Li S, Sawh S, Muley A, Ishii J, et al. Extracellular vesicles in DLBCL provide abundant clues to aberrant transcriptional programming and genomic alterations. Blood. 2018;132:e13–e23.
22. Feng Y, Zhong M, Zeng S, Wang L, Liu P, Xiao X, et al. Exosome-derived miRNAs as predictive biomarkers for diffuse large B-cell lymphoma chemotherapy resistance. Epigenomics. 2019;11:35–51.
23. Vega JA, García-Suárez O, Hannestad J, Pérez-Pérez M, Germanà A. Neurotrophins and the immune system. J Anat. 2003;203:1–19.
24. Griffin N, Faulkner S, Jobling P, Hondermarck H. Targeting neurotrophin signaling in cancer: the renaissance. Pharmacol Res. 2018;135:12–17.
25. Bellanger C, Dubanet L, Lise MC, Fauchais AL, Bordessoule D, Jauberteau MO, et al. Endogenous neurotrophins and Trk signalling in diffuse large B cell lymphoma cell lines are involved in sensitivity to rituximab-induced apoptosis. PLoS ONE. 2011;6:e27213.
26. Dubanet L, Bentayeb H, Petit B, Olivrie A, Saada S, de la Cruz-Morcillo MA, et al. Anti-apoptotic role and clinical relevance of neurotrophins in diffuse large B-cell lymphomas. Br J Cancer. 2015;113:934–44.
27. Jang SW, Liu X, Yepes M, Shepherd KR, Miller GW, Liu Y, et al. A selective TrkB agonist with potent neurotrophic activities by 7,8-dihydroxyflavone. Proc. Natl Acad Sci USA. 2010;107:2687–92.
28. Théry C, Amigorena S, Raposo G, Clayton A. Isolation and characterization of exosomes from cell culture supernatants and biological fluids. Curr Protoc Cell Biol. 2006;Chapter 3:Unit 3.22
29. Théry C, Witwer KW, Aikawa E, Alcaraz MJ, Anderson JD, Andriantsitohaina R, et al. Minimal information for studies of extracellular vesicles (MISEV2018): a position statement of the International Society for Extracellular Vesicles and update of the MISEV2014 guidelines. J Extracell Vesicles. 2018;7:1535750.
30. Bentayeb H, Aitamer M, Petit B, Dubanet L, Elderwish S, Désaubry L, et al. Prohibitin (PHB) expression is associated with aggressiveness in DLBCL and flavagline-mediated inhibition of cytoplasmic PHB functions induces anti-tumor effects. J Exp Clin Cancer Res. 2019;38:450
31. Bentayeb H. Résistances/sensibilisations aux anti-CD20 (rituximab) dans les lymphomes diffus à grandes cellules B (DLBCL). Méd Hum Pathol. 2016; https://tel.archives-ouvertes.fr/tel-01957664/document.
32. Xia B, Li M, Yang R, Wang X, Shun C, Zhang Y. The central roles of exosomes in hematological malignancies: a new frontier review. Biosc Biotech Res Commun. 2018;11:1–4.
33. Fernandes M, Teixeira AL, Medeiros R. The opportunistic effect of exosomes on Non-Hodgkin Lymphoma microenvironment modulation. Crit Rev Oncol Hematol. 2019;144:102825
34. Olejniczak SH, Stewart CC, Donohue K, Czuczman MS. A quantitative exploration of surface antigen expression in common B-cell malignancies using flow cytometry. Immunol Invest. 2006;35:93–114.
35. Johnson NA, Boyle M, Bashashati A, Leach S, Brooks-Wilson A, Sehn LH, et al. Diffuse large B-cell lymphoma: reduced CD20 expression is associated with an inferior survival. Blood. 2009;113:3773–80.
36. Oksvold MP, Kullmann A, Forfang L, Kierulf B, Li M, Brech A, et al. Expression of B-cell surface antigens in subpopulations of exosomes released from B-cell lymphoma cells. Clin Ther. 2014;36:847–862.e1.
37. Tomita A. Genetic and epigenetic modulation of CD20 expression in B-cell malignancies: molecular mechanisms and significance to rituximab resistance. J Clin Exp Hematop. 2016;56:89–99.
38. Arévalo JC, Wu SH. Neurotrophin signaling: many exciting surprises!. Cell Mol Life Sci. 2006;63:1523–37.

39. Wojciechowski W, Li H, Marshall S, Dell'Agnola C, Espinoza-Delgado I. Enhanced expression of CD20 in human tumor B cells is controlled through ERK-dependent mechanisms. J Immunol. 2005;174:7859–68.
40. Winiarska M, Bojarczuk K, Pyrzynska B, Bil J, Siernicka M, Dwojak M, et al. Inhibitors of SRC kinases impair antitumor activity of anti-CD20 monoclonal antibodies. MAbs. 2014;6:1300–13.
41. Escudero CA, Lazo OM, Galleguillos C, Parraguez JI, Lopez-Verrilli MA, Cabeza C, et al. The p75 neurotrophin receptor evades the endolysosomal route in neuronal cells, favouring multivesicular bodies specialised for exosomal release. J Cell Sci. 2014;127:1966–79.
42. Ishii T, Warabi E, Mann GE. Circadian control of BDNF-mediated Nrf2 activation in astrocytes protects dopaminergic neurons from ferroptosis. Free Radic Biol Med. 2019;133:169–78.
43. Zare N, Haghjooy Javanmard SH, Mehrzad V, Eskandari N, Andalib AR. Effect of plasma-derived exosomes of refractory/relapsed or responsive patients with diffuse large B-cell lymphoma on natural killer cells functions. Cell J. 2020;22:40–54.

AUTHOR CONTRIBUTIONS

Conception and design: DT and HB. Acquisition, analyse and interpretation of data: MA, HB, MB, CV and DT; drafting the article or revising it critically for important intellectual content: DT, HB and HA; wrote the paper including design of figures: DT, MA and HB; final approval of the version to be published: DT, M-OJ, NG, JF, JA and HS.

FUNDING

This work was supported by grants from Institut Roche, Région Nouvelle Aquitaine, Ligue Contre le Cancer (87) and CORC (Comité d'Orientation Recherche Cancer en Limousin).

COMPETING INTERESTS

The authors declare no competing interests.

ETHICS APPROVAL AND CONSENT TO PARTICIPATE

All procedures involving animals were carried out in accordance with the standards approved by the internal Institutional Animal Care and Use Committee (CREEAL No. 2-07-2012).

ADDITIONAL INFORMATION

Supplementary information The online version contains supplementary material available at https://doi.org/10.1038/s41416-021-01611-7.

Correspondence and requests for materials should be addressed to Danielle Troutaud.